

Direct Deposit of Fiber Reinforced Energetic NanoComposites**

Xiangyu Li^[a] and Michael R. Zachariah^{*,[a]}

Abstract: The ideal situation of assembling an energetic nanoparticles-polymer matrix is obtaining materials with high particle loading while still maintaining mechanical integrity. In this paper, we introduced a direct deposition approach to create a reactive polymer fiber reinforced composite with aluminum (Al-NPs) and copper oxide nanoparticles (CuO-NPs) in a polyvinylidene fluoride (PVDF) reactive binder. Even with up to 70 wt% thermite, these films still maintain a uniform morphology and considerable flexibility. With the same overall material composition, both the reactive and mechanical properties of fiber reinforced films shown marked improvement over the corresponding non-nano-

fiber films. The combustion propagation velocity of fiber reinforced films is up to 1.8 times faster than the corresponding non-nanofiber films. For the mechanical properties, the films with 110 nm diameter fibers were 2.3, 23 and 5.8 times superior in tensile strength, strain and toughness respectively, as compared to films with the same mass loading but with no fibers. The results suggest deploying a fiber reinforced structure enables fabrication of nanocomposite with high loadings of energetic materials. These result imply that a 3-D printing approach may demonstrate significant advantages in developing advanced propulsion systems.

Keywords: nano-composite · nanofiber · electrospray · additive manufacturing

1 Introduction

Nanothermite, a class of highly reactive energetic material, usually consists of two components: a fuel – nanometer scale metal particles e.g. Al, Mg, Si and B; an oxidizer – nanoscale metal oxide like CuO, Fe₂O₃. Thermite reactions are self-sustaining, deliver higher energy density and higher adiabatic reaction temperatures than CHNO systems [1–4]. The use of nanoscale reactants enables superior combustion performance than the conventional micro counterparts, due to the decreased diffusion distances and increased interfacial contact. For example, mixtures of Al and MoO₃ nanoparticles (average particle sizes ~20–50 nm) were found to react more than 1000× faster than a traditional microthermite [5,6]. Thus far, most studies related to nanothermites have focused on the fuel-oxidizer system itself. However, in some potential applications (e.g. the biocidal agents [7], cloud-seeding material [8]), the thermite powder were incorporated with polymer binders (epoxy, nitrocellulose, and fluoropolymer [9–14]) to form the nanothermite-polymer composites. A large content of thermite is nominally desirable since it is the dominate energy releasing source, while the polymer binder is employed to give the composite the necessary mechanical integrity. However, at high loadings of nanothermite, making a homogeneous composite is difficult due to processing constraints in mixing constituents.

In part, the formulation of polymer composites with high mass loading of nanoparticles is virtually impossible because of the high viscosity of polymer binder and nano-

meter-scale fuel/oxidizer mixture [15,16]. As our previous work reported, polymer nanocomposite with small amounts of nanostructured material usually demonstrate better mechanical integrity than the pure polymer, however, higher loadings of nanomaterial result in heavy aggregation [17–19]. The aggregation of fuel/oxidizer nanoparticles eventually leads to the degradation of the composite for both its reactive and mechanical properties [20].

Deploying a fiber reinforced structure can significantly enhance the mechanical strength of the composite, which can be realized by embedding high-strength fibers, such as aramid, glass and carbon [21] into a polymer matrix. In this manner, the particle loading – mechanical strength dilemma may be solved within such a structure.

In this work an energetic nanofiber reinforced composite was employed to improve both the reactive and mechanical properties of the nanothermite-polymer compo-

[a] X. Li, Prof. M. R. Zachariah
Department of Chemical Engineering and Biomolecular Engineering
Department of Chemistry and Biochemistry
University of Maryland, College Park, 20742, USA
*e-mail: mrz@umd.edu

[**] This work was supported by an AFOSR grant. We acknowledge the support of the Maryland Nanocenter and its NispLab. The NispLab is supported in part by the NSF as a MRSEC Shared Experimental Facility. Xiangyu Li is grateful for the financial support from Nanjing University of Science and Technology. (Supporting Information is available online from Wiley InterScience).

 Supporting information for this article is available on the WWW under <https://doi.org/10.1002/prop.201700038>

site. Al-NPs/CuO-NPs nanothermite was chosen as the fuel/oxidizer solids to be studied. We choose a fluorine containing polymer (polyvinylidene fluoride, PVDF) as a reactive binder due to its strong oxidation nature.

We employed a combined electrospinning and electro-spray method to fabricate the energetic fiber reinforced composite. Electrospinning and electro-spray are closely related methods that have been shown as effective methods to produce composite nanofibers and thin films [22–24]. In both cases, high electric fields are employed to produce a charged liquid jet emanating from a Taylor cone. In electro-spray, the electrostatic force is greater than the molecular cohesive force of the liquid (i.e. surface tension), leading to jet breakup to form charged droplets. In electrospinning, jet breakup does not occur due to high loadings of polymer, so that a continuous fiber can be extruded [25,26].

Both methods offer considerable control through process parameters. Parameters like solution surface tension, electrical conductivity and flow rate, can be used to control drop size which typically is monomial due to coulombically driven droplet fissions [27–31]. Most importantly, the polymer solution used may contain a dispersion of nanoparticles, which remain within the droplets as the precursor jet undergoes break up. The solvent in the fine charged droplets rapidly evaporate as they are extracted and accelerated by the extracting electric field, leaving concentrated nanoparticles and polymer, which were finally collected onto a substrate to create a uniform, high nanoparticle loading polymer composite. Fibers drawn from electrospinning act in a similar way with fiber diameter controlled by the solution surface tension and electrical conductivity. To create a fiber reinforced films we build on our prior work in the use of electro-spray deposition as a simple technique to produce laminate high nanoparticle loadings nano-composites [32]. The fiber reinforced films are composed of Al/CuO nanothermites, which is the most commonly used combination, incorporated with a PVDF reactive binder, with PVDF nanofibers embedded within. These results show that nanofiber reinforced structure can significantly enhance both the reactive and mechanical properties of the energetic nanocomposite.

2 Materials and Methods

2.1 Materials

Al-NPs, (average particle size: 50 nm, purity: 70 wt % [32,36]) were purchased from Argonide Corporation, CuO-NPs (purity: 99.8 wt %, average particle size: 30 nm), Ammonium perchlorate (AP) (purity: 99.8 wt %), PVDF (Molecular weight: 534,000) and Dimethylformamide (DMF) (purity: 99.8 wt %) were purchased from Sigma–Aldrich.

2.2 Precursor Preparation

A PVDF (10.4 wt %)-DMF (32.4 wt %)-acetone (57.2 wt %) solution was used as the precursor for the PVDF nanofiber. And the precursor for forming the Al-NPs/CuO-NPs thermite matrix included 4.3 wt % of PVDF dissolved in 81.9 wt % DMF, to which 7.7 wt % of CuO-NPs and 6.2 wt % of Al-NPs was added into the PVDF-DMF solution. In addition, 0.12 wt % of AP was added to increase the electrical conductivity of the mixture, so that a dense film could be deposited by the stabilized spray [32]. Thirty minutes of magnetic stirring of the mixture was used to disperse the nanoparticles, followed by one hour of ultrasonication. Finally the suspension was magnetically stirred for another 24 hours at room temperature.

2.3 Electro-spray and Electrospinning Deposition

As demonstrated in Figure 1, both electrospinning and electro-spraying were employed in fabricating PVDF nanofiber and the thermite matrix, respectively. A home-made two-needle spray setup was employed to create the film. Precursors for nanofiber and matrix were separately pumped through two stainless steel tubes (0.023 mm inner diameter) and sprayed toward a rotating collector with ground potential, enabling the embedding of nanofiber within the matrix. The needle tip for electrospinning was placed 10 cm away from the collector while the electro-spray needle was placed 6 cm away. The same working voltage of 18 kV was applied to both needles. In the experiment, fine droplets from electro-spray were collected wet to form the matrix and nanofibers from electrospinning were collected dry as reinforcement. Flow rates of 0.5–1.5 ml h⁻¹ were applied in the electrospinning process to obtain fibers with an average diameter of 110 to 230 nm. The flow rate for the electro-spray process was adjusted accordingly to vary the matrix mass loading of the film. After the electrospinning/electro-spray process, the prepared film was carefully peeled off.

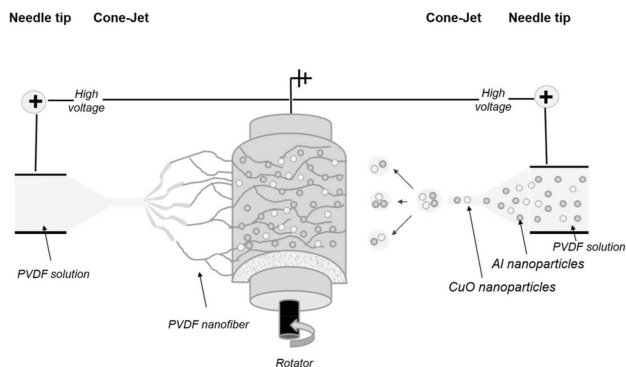


Figure 1. Electro-spray/electrospinning deposition process for fabricating PVDF nanofiber reinforced films.

2.4 Characterization

We chose combustion propagation velocity as a suitable metric to evaluate reactive behavior using a homemade combustion test setup. The detailed procedure could be found in our previous work (Support information Figure S1) [32,36].

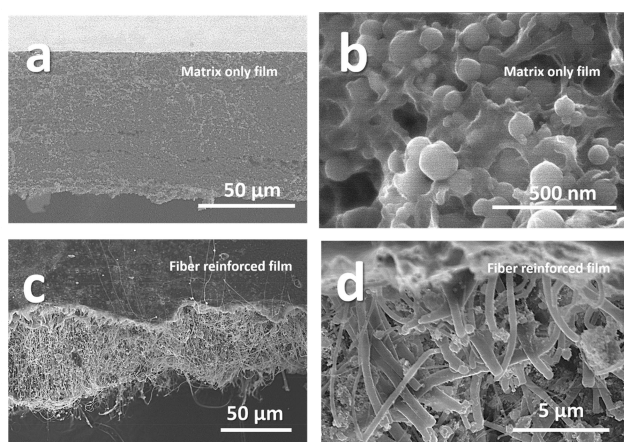
The morphologies and thickness of the fiber-reinforced films were characterized by scanning electron microscopy (SEM, Hitachi, SU-70 FEG-SEM). The sample preparation process could also be found in the previous work [36].

We used a home-made micro-tensile tester [33,36] to study the mechanical properties of the films. Each film was tested three times using strip specimens (2.5 cm × 0.5 cm) for an accurate result. The initial thickness and width were respectively obtained by SEM and a digital caliper before each test. The parameter of the micro-tensile tester was same as the some of our previous work [36], with more details provided in the supplement material.

3 Results and Discussion

3.1 Morphology Characteristics

SEM images of the as prepared fibers and films are shown in Figure 2. The standalone Al-NPs/CuO-NPs/PVDF thermite film (The matrix, Figure 2a) shows a dense, crack-free con-



Nano-Fibers were embedded within the thermite matrix

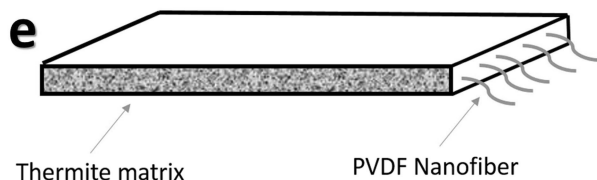


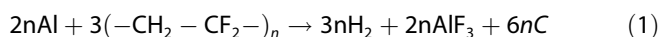
Figure 2. Cross-sectioned SEM images (a) and (b) of Al-NPs/CuO-NPs/PVDF thermite matrix only film; (c) and (d) fracture section of the fiber reinforced film (21.1 wt% PVDF nanofiber, average fiber diameter 110 nm). (e) An illustration of the fiber reinforced film.

stant thickness nanoparticle-polymer film. From the high magnification image (Figure 2b), we see that the nanoparticles were evenly distributed among and connected by the PVDF polymer network, indicating a successful fabrication of high nanoparticle loading polymer composite. Figure 2c is the fracture section of the fiber reinforced film which contains 21.1% PVDF nanofiber (40 wt% total PVDF, average fiber diameter 110 nm). Smooth nanofibers were heavily packed and protruded out from the fracture section of the thermite film, indicating that those fibers were successfully embedded within the thermite matrix (Figure 2d and e).

3.2 Reactive Properties

Films containing different mass loading of PVDF nanofibers but with the same average fiber diameter were prepared to investigate the reactive properties of the fiber reinforced films. All samples were cut to 2.5 × 0.5 cm strips, and ignited by a hot Ni–Cr wire under ambient argon within a Plexiglas enclosure. The burning rate was measured parallel to the rotation direction of the collector (parallel to the reinforced fiber). Thus in principle at least the fiber can act as a thermal conductor in the direction of propagation. The combustion process were recorded by a high speed camera for further analysis. In addition to the PVDF that already resides in the matrix, 0 to 21.1 wt% of PVDF nanofiber was added into the Al/CuO/PVDF thermite matrix (24 wt% PVDF, 33 wt% Al-NPs, and 43 wt% CuO-NPs), resulting in a fiber reinforced film with a total PVDF mass ratio of between 24 to 40 wt%. In all cases, the embedded nanofibers have the same average diameter of ~110 nm.

In our earlier work we proposed the following global reactions [32,36]:



In all experiments, the PVDF/Al/CuO molar ratio of the thermite matrix was fixed at 0.5/1.1/0.7. According to equation (1) and (2), the complete reaction requires a PVDF/Al/CuO molar ratio of 1.0/1.1/0.7, indicating a fuel-rich composition for the matrix formula [36]. For each fiber reinforced film, a film without PVDF nanofiber but with same total material composition was also prepared for comparison. The total PVDF mass ratio, the stoichiometry of the whole film, matrix mass ratio and PVDF nanofiber mass ratio of as-prepared fiber reinforced and non-nanofiber films are listed in Table 1.

Both the fiber reinforced and non-nanofiber films could be easily ignited by the hot Ni–Cr wire under argon, showing a stable and complete propagating combustion process. The average combustion velocity are shown in Figure 3. It should be noted that the left most (No fiber) data point is

Table 1. Properties of fabricated films:

	Total PVDF[a] (including fiber) [wt%]	Molar Ratio ^a PVDF/Al/CuO	Matrix mass [wt%]	PVDF Nanofiber [wt%]
Fiber reinforced film	30	0.67/1.1/0.7	91.1	8.9
	35	0.84/1.1/0.7	85.5	14.5
	40	1.04/1.1/0.7	78.9	21.1
	PVDF mass ratio [wt%]	Molar Ratio ^a PVDF/Al/CuO		
Non-nanofiber film	24	0.5/1.1/0.7		
	30	0.67/1.1/0.7		
	35	0.84/1.1/0.7		
	40	1.04/1.1/0.7		

[a] Assuming PVDF unit formula is $C_2H_2F_2$

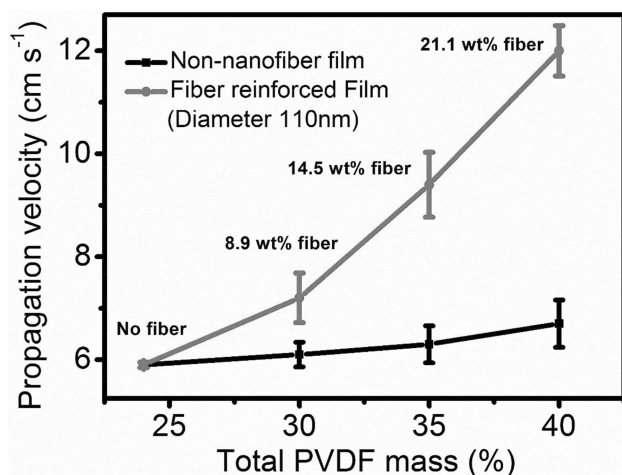


Figure 3. Average propagation velocity of fiber reinforced and single layer thermite film as a function of PVDF mass (including PVDF in fibers), when the PVDF nanofiber diameter is fixed at 110 nm. Particle concentration in matrix is fixed in all fiber reinforced films.

the film with 24 wt% PVDF, is a nanofiber free film (thermite matrix). The propagation velocity vs PVDF mass ratio curves of both kinds of films have the similar basic trend. For both the fiber reinforced and corresponding non-nanofiber films, increasing PVDF mass ratio leads to a faster burn rate. Films with 40 wt% PVDF shows the fastest burning rate in argon. The result is reasonable since the overall material composition of the film is approaching stoichiometry (Table 1) as we are increasing the total PVDF mass ratio. *Meanwhile, even*

though the overall material composition was exactly the same in both types of films, the fiber reinforced films still demonstrate a higher combustion velocity in argon.

In our case, the porosity of the fiber reinforced films and the corresponding non-nanofiber films show no obvious difference (the porosity of both films were between 33–38%), support information Figure S2). This indicates that the porosity of the film has little influence on the reactive property difference.

It is widely accepted that the intimacy between fuel and oxidizer is an important factor that influence the combustion performance of energetic composite materials.^[34,35] It is easy to conceptualize that the inter-particle distance in the non-nanofiber film is larger than that of fiber reinforced films for the same total PVDF loading (Support information, Figure S3). By adding PVDF nanofiber instead of mixing PVDF homogeneously, we can vary the overall equivalence ratio while maintaining the same inter-particle distance. Thus in the case shown in Figure 3, increasing fiber content increased burn rate but had the same effective interparticle spacing. Comparing the fiber reinforced vs the nonfiber reinforced case at the same PVDF loading, one can see that the absence of fibers leads to increased particle spacing.

The reactive properties of fiber reinforced films, employing the same mass ratio of nanofibers, but with different average diameter were also investigated. PVDF nanofibers with average diameter of ~110 nm, 190 nm, and 240 nm were deposited into the matrix (24 wt% PVDF, 33 wt% Al-NPs and 43 wt% CuO-NPs, respectively). The mass ratio of PVDF nanofiber and total PVDF in all samples were fixed at 21.1% and 40 wt%, respectively. Figure 4 shows a monotonic decrease in propagation velocity with increasing fiber diameter. The result seems reasonable because the fiber with smaller diameter also has the larger specific surface area. For the same mass of PVDF, the 110 nm fibers have a

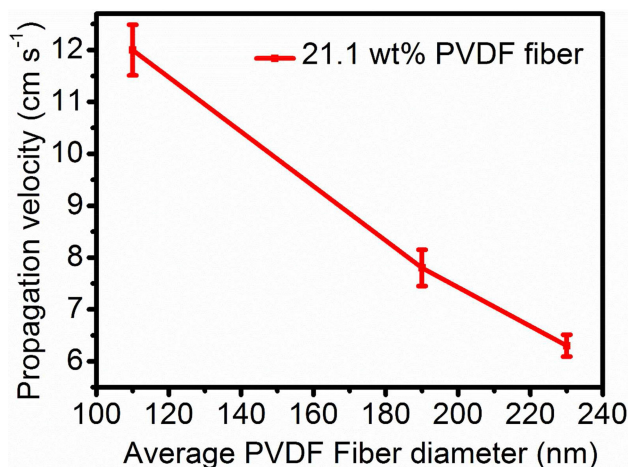


Figure 4. Effect of fiber diameter on combustion propagation velocity. Films contained the PVDF nanofiber loading but different average fiber diameter.

2.1 × larger surface area than 230 nm case, which indicates that a more intimate interfacial contact was achieved between the PVDF nanofiber and matrix. In all cases, faster burning was observed in the films with thinner PVDF fibers.

3.3 Mechanical Performance

One of the major challenges in high particle loading polymer composites is maintaining mechanical integrity. To evaluate the potential advantages of nanofiber reinforced composites, two groups of films were prepared.

Group 1: Fiber reinforced films with differing mass loading of PVDF nanofiber, but with the same average fiber diameter (110 nm). Evaluate effect of fiber loading (Same as the fiber reinforced films presented in Table 1).

Group 2: Fiber reinforced films with 40 wt% total PVDF (21.1 wt% PVDF nanofiber) but different average fiber diameter. Films without fibers contained 40 wt% total PVDF (Same as the non-nanofiber films presented in Table 1).

Figure 5 shows the stress-strain behavior of samples from group 1 (i.e. effect of fiber loading), and demonstrates that the films with higher loadings of PVDF nanofibers show better mechanical performance. As the nanofiber mass fraction increased from 0 to 21.1 wt%, the tensile strength (Figure 5a), strain (Figure 5b) and toughness (Figure 5c) showed a 130%, 520% and 1430% improvement.

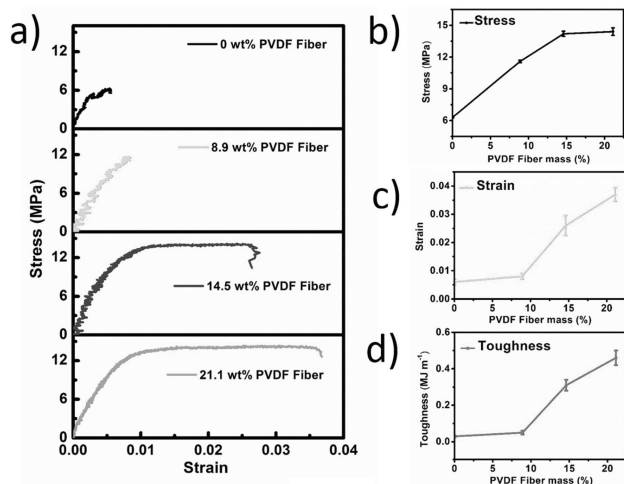


Figure 5. Group 1; Effect of Fiber Mass Loading: Stress–strain curves (a), tensile stress (b), strain (c) and toughness (d) as a function of total PVDF mass (group 1): Fiber reinforced films with different amount of PVDF nanofiber but same average fiber diameter. All samples have the same average fiber diameter (110 nm).

The effect of fiber diameter (group 2) was evaluated by holding the total PVDF loading at 40 wt%. From Figure 6 it is quite clear that thinner fibers lead to better mechanical performance. Films with 110 nm diameter fibers were 1.6, 1.8 and 2.9 times better in tensile strength (Figure 6a), strain (Fig-

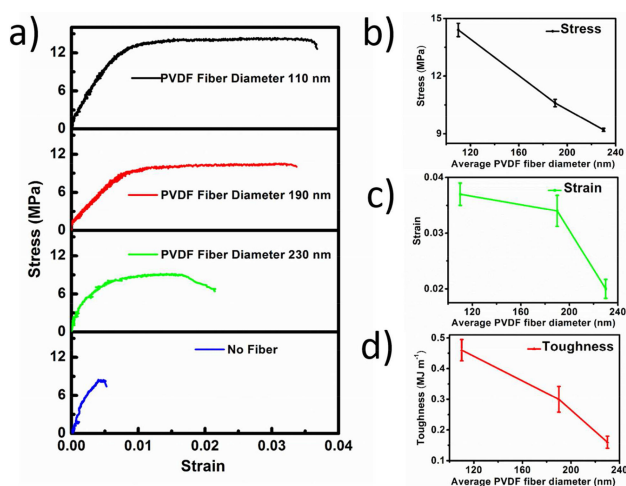


Figure 6. Group 2; Effect of Fiber Diameter: Stress–strain curves (a), tensile stress (b), strain (c) and toughness (d) as a function of total PVDF mass (group 2): Fiber reinforced films with same amount of PVDF nanofiber but different average fiber diameter. : Fiber reinforced films with 40 wt% total PVDF (21.1 wt% PVDF nanofiber).

ure 6b) and toughness (Figure 6c) respectively as compared to films with the same mass loading but with 230 nm diameter fibers. Moreover, all films with nanofiber show better mechanical performance as compared to films with the same mass loading but with no fibers. The biggest enhancements were for the smallest fibers; 110 nm diameter fibers; where the tensile strength, strain and toughness were 2.3, 2.3 and 5.8 times better as compared to their non-fibers counterparts. The result clearly shows that higher particle loading can be achieved in a fiber reinforced nanocomposite as compared to the same non-fiber counterpart, and offers an opportunity to achieve very high particle loadings.

Our previous work shows that pure PVDF (tensile strength: 18 MPa, strain 110%, toughness: 19 MJ m⁻³) has superior mechanical performance than the matrix film [32], which can act as a reinforcement for the thermite layer matrix when fabricated in a laminate form [36]. Here, part of the load applied on the weak matrix can be transferred onto the strong nanofiber reinforcement through the interface between them. More PVDF nanofiber (reinforcement) with the same average diameter means more load can be transferred from the matrix to the reinforcement. As for films with the same amount of PVDF nanofiber but different fiber diameter, films with thinner fibers have a larger interfacial area between the reinforcement and the matrix which leads to a more effective load transfer at constant fiber loading.

4 Conclusions

We demonstrated a direct deposition process to successfully fabricate PVDF nanofiber reinforced nanothermite polymer films. Experimental results show that nanofiber re-

inforced structures improved the reaction properties, which correlated with decreasing fiber diameter. Fiber reinforced films also show considerably better mechanical integrity, and indicate that the particle loadings (up to 70 wt% nanoparticles)-mechanical strength dilemma can be solved by deploying this structure. The general structure offers an opportunity to introduce high nanoparticle loadings propellant grain with high mechanical integrity.

References

- [1] R. A. Yetter, G. A. Risha, S. F. Son, Metal particle combustion and nanotechnology, *P. Combust. Inst.* **2009**, *32*, 1819.
- [2] P. Brousseau, C. J. Anderson, Nanometric Aluminum in Explosives, *Propell. Explos. Pyrot.* **2002**, *27*, 300.
- [3] A. A. Gromov, U. Teipel, *Metal Nanopowders: Production, Characterization, and Energetic Applications*, Wiley, **2014**.
- [4] V. N. Krishnamurthy, S. Thomas, *Defence Sci. J.* **1987**, *37*, 29.
- [5] E. L. Dreizin, Metal-based reactive nanomaterials, *Prog. Energ. Combust. Sci.* **2009**, *35*, 141.
- [6] A. Jaworek, Electro spray droplet sources for thin film deposition, *J. Mater. Sci.* **2007**, *42*, 266.
- [7] X. Hu, J. B. DeLisio, X. Li, M. R. Zachariah, Direct deposit of highly reactive $\text{Bi}(\text{IO}_3)_3$ polyvinylidene fluoride biocidal energetic composite and its reactive properties, *Adv. Eng. Mater.*, DOI: 10.1002/adem.201500532.
- [8] X. Hu, W. Zhou, X. Wang, T. Wu, J. B. DeLisio, M. R. Zachariah, On-the-fly green generation and dispersion of AgI nanoparticles for cloud seeding nuclei, *J. Nanopart. Res.* **2016**, *18*, 214.
- [9] S. Yan, G. Jian, M. R. Zachariah, Electro spun nanofiber-based thermite textiles and their reactive properties, *ACS Appl. Mater. Inter.* **2012**, *4*, 6432.
- [10] X. Li, X. Liu, Y. Cheng, Y. Li, X. Mei, Thermal decomposition properties of double-base propellant and ammonium perchlorate, *J. Therm. Anal. Calorim.* **2014**, *115*, 887.
- [11] H. A. Miller, B. S. Kusel, S. T. Danielson, J. W. Neat, E. K. Avjian, S. N. Pierson, S. M. Budy, D. W. Ball, S. T. Iacono, S. C. Kettwich, Metastable nanostructured metallized fluoropolymer composites for energetics, *J. Mater. Chem. A* **2013**, *1*, 7050.
- [12] E. C. Koch, *Metal-Fluorocarbon Based Energetic Materials*, John Wiley & Sons, **2012**.
- [13] D. W. Smith, S. T. Iacono, D. J. Boday, S. C. Kettwich, *Advances in Fluorine-Containing Polymers*, American Chemical Society, **2012**.
- [14] J. B. DeLisio, X. Hu, T. Wu, G. C. Egan, G. Young, M. R. Zachariah, Probing the reaction mechanism of Aluminium/Poly (vinylidene fluoride) Composites, *J. Mater. Chem. B* **2016**, *120*, 24.
- [15] L. Meda, G. Marra, L. Galfetti, S. Inchingalo, F. Severini, L. De Luca, Nano-composites for rocket solid propellants, *Compos. Sci. Technol.* **2005**, *65*, 769.
- [16] L. Galfetti, L. De Luca, F. Severini, L. Meda, G. Marra, M. Marchetti, M. Regi, S. Bellucci, Nanoparticles for solid rocket propulsion, *J. Phys.: Condens. Matter.* **2006**, *18*, S1991.
- [17] G. V. Kumar, C. Rao, N. Selvaraj, Mechanical and tribological behavior of particulate reinforced aluminium metal matrix composites – a review, *J. Miner. Mater. Charact. Eng.* **2011**, *10*, 59.
- [18] Y. Xu, S. H. Van, Mechanical properties of carbon fiber reinforced epoxy/clay nanocomposites, *Compos. Sci. Technol.* **2008**, *68*, 854.
- [19] T. Sekitani, Y. Noguchi, K. Hata, T. Fukushima, T. Aida, T. Someya, A rubberlike stretchable active matrix using elastic conductors, *Science* **2008**, *321*, 1468.
- [20] W. Zuiderduin, C. Westzaan, J. Huetink, R. Gaymans, Toughening of polypropylene with calcium carbonate particles, *Polymer* **2003**, *44*, 261.
- [21] H. Ku, H. Wang, N. Pattarachaiyakoop, M. Trada, A review on the tensile properties of natural fiber reinforced polymer composites, *Composites Part B* **2011**, *42*, 856.
- [22] D. G. Piercey, T. M. Klapoetke, Cent. Eur. Nanoscale aluminium-metal oxide (thermite) reactions for application in energetic materials, *J. Energ. Mater.* **2010**, *7*, 115.
- [23] Y. Xu, Y. Zhu, F. Han, C. Luo, C. Wang, 3D Si/C fiber paper electrodes fabricated using a combined electrospray/electrospinning technique for Li-ion batteries, *Adv. Energy Mater.* **2015**, *5*.
- [24] I. B. Rietveld, K. Kobayashi, H. Yamada, K. Matsushige, Process parameters for fast production of ultra-thin polymer film with electrospray deposition under ambient conditions, *J. Colloid. Interface Sci.* **2009**, *339*, 481.
- [25] D. Li, Y. N. Xia, Electrospinning of nanofibers: reinventing the wheel? *Adv. Mater.* **2004**, *16*, 1151.
- [26] A. Greiner, J. H. Wendorff, Electrospinning: a fascinating method for the preparation of ultrathin fibers, *Angew. Chem. Int. Ed.* **2007**, *46*, 5670.
- [27] J. Fernandez, De La Mora, J. Navascues, F. Fernandez, J. Rosell-Llompart, Generation of submicron monodisperse aerosols in electrosprays, *J. Aerosol. Sci.* **1990**, *21*, S673.
- [28] D. La Mora, J. Fernández, The effect of charge emission from electrified liquid cones, *J. Fluid. Mech.* **1992**, *243*, 561.
- [29] G. Meesters, P. Vercoulen, J. Marijnissen, B. Scarlett, Generation of micron-sized droplets from the Taylor cone, *J. Aerosol. Sci.* **1992**, *23*, 37.
- [30] D. La Mora, J. Fernandez, The current emitted by highly conducting Taylor cones, *J. Fluid. Mech.* **1994**, *260*, 155.
- [31] M. Gamero-Castano, I. Aguirre-de-Carcer, L. De Juan, J. F. de la Mora, On the current emitted by Taylor cone-jets of electrolytes in vacuo: Implications for liquid metal ion sources, *J. Appl. Phys.* **1998**, *83*, 2428.
- [32] C. Huang, G. Jian, J. B. DeLisio, H. Wang, M. R. Zachariah, Electro spray deposition of energetic polymer nanocomposites with high mass particle loadings: a prelude to 3d printing of rocket motors, *Adv. Eng. Mater.*, DOI: 10.1002/adem.201400151.
- [33] A. L. Gershon, D. P. Cole, A. K. Kota, H. A. Bruck, Nano-mechanical characterization of dispersion and its effects in nano-enhanced polymers and polymer composites, *J. Mater. Sci.* **2010**, *45*, 6353.
- [34] K. T. Sullivan, N. W. Piekielek, C. Wu, S. Chowdhury, S. T. Kelley, T. C. Hufnagel, K. Fezzaa, M. R. Zachariah, Reactive sintering: An important component in the combustion of nanocomposite thermites, *Combust. Flame.* **2012**, *159*, 2.
- [35] K. T. Sullivan, W. A. Chiou, R. Fiore, M. R. Zachariah, In situ microscopy of rapidly heated nano-Al and nano-Al/WO₃ thermites, *Appl. Phys. Lett.* **2010**, *97*, 133104.
- [36] X. Li, P. Guerieri, W. Zhou, C. Huang, M. R. Zachariah, Direct deposit laminate nanocomposites with enhanced propellant properties, *ACS Appl. Mater. Interfaces.* **2015**, *7*, 9103.

Received: February 2, 2017

Revised: May 30, 2017

Published online: July 7, 2017